EPJ Web of Conferences **95**, 04061 (2015)
DOI: 10.1051/epjconf/20159504061

Search for heavy resonances with the ATLAS detector

Natascha Schuh[1,a], on behalf of the ATLAS Collaboration
[1]*Johannes Gutenberg University Mainz*

Abstract. The ATLAS detector at the Large Hadron Collider (LHC) is used to search for heavy resonances in various final states. Recent results from different analyses of the proton-proton (pp) collisions recorded in 2012 at a center-of-mass energy of $\sqrt{s}$ =8 TeV corresponding to an integrated luminosity of $L_{int} \approx 20\,\text{fb}^{-1}$ are presented. Various models are considered such as W′ and Z′ bosons, chiral bosons, excited quarks and technicolor, as well as a Randall-Sundrum graviton, the ADD large extra dimension scenario, (quantum) black holes and contact interactions.

1 Introduction

The Large Hadron Collider (LHC) [1] is with a length of 27 km the world's largest circular accelerator. On the basis of proton-proton (pp) collisions, it provides the possibility to look into totally new and undiscovered energy regions. Located at CERN[1] nearby Geneva, Switzerland, the LHC is used by four major experiments. With a length of 44 m, a diameter of 25 m and a mass of 7000 t, the ATLAS[2] detector [2] is the largest of these four. The huge amount of pp collision data with an integrated luminosity of about $L_{int} \approx 20\,\text{fb}^{-1}$ collected at a center-of-mass energy of $\sqrt{s}$=8 TeV with the ATLAS detector during 2012 allows to exploit the LHC as a discovery machine and to search for answers to the remaining questions that are not considered within the Standard Model of particle physics (SM). Various models provide possible extensions and new physics scenarios resulting in distinct experimental signatures are examined. Looking into different analysis channels, many searches for resonances or deviations from well understood SM expectations are performed.

[a]e-mail: Natascha.Schuh@cern.ch
[1]**C**onseile **E**uropéen pour la **R**echerche **N**ucléaire <fr.>, European Council of Nuclear Research
[2]**A** **T**oroidal **L**hc **A**pparatu**S**

2 Searches for new physics

2.1 Search for heavy resonances in final states with one lepton plus missing transverse energy

Searching for new physics scenarios in final states with one lepton plus missing transverse energy, two different extending theories are considered [3]. A first possible extension to the SM is provided by the Sequential Standard Model (SSM) predicting additional heavier vector gauge bosons with spin-1 outside the SM, denoted as W′ (charged current) and Z′ (neutral current). Their couplings to SM fermions are assumed to be identical to those of the SM bosons whereas couplings to W/Z (in the W′ case) are set to zero. The intrinsic width of the resonance increases linearly with the boson mass, and is assumed small compared to the detector resolution. An interference with the SM W or Z is neglected in the analysis.
The second model considers chiral bosons, denoted as W* in the charged and Z* in the neutral case. These electroweak doublet spin-1 vector bosons are mainly motivated by the hierarchy problem and predicted by at least three theories explaining the relative lightness of the Higgs doublets (namely the pseudo-Goldstone Higgs, the Goldstone Sister Higgs and the Higgs as Extra Dimensional Gauge Field). Their anomalous (magnetic moment type) couplings to SM fermions differ from SM couplings and result in significantly different kinematic distributions.

Selecting events with one high transverse momentum lepton (electron or muon) and high missing transverse energy, it is possible to reconstruct the so-called transverse mass $m_T = \sqrt{2p_T E_T^{miss}(1-\cos\phi_{l\nu})}$ that is used as signal discriminant. The transverse momentum of the lepton is denoted as p_T, E_T^{miss} is the magnitude of the missing transverse energy vector and $\phi_{l\nu}$ denotes the angle between the p_T and E_T^{miss} vectors.
The dominant and irreducible background contribution comes from SM W decays to the same final state. The next largest that can have real E_T^{miss} and isolated leptons arises due to diboson (WW, WZ, ZZ) decays, followed by $t\bar{t}$ and single top production which is most important for the lowest W′ or W* pole masses. Z boson decays where one lepton could not be reconstructed and is therefore mimicking real E_T^{miss} result in a minor background contribution. Strong-interaction processes such as heavy-flavour decays or misidentification of jets as electrons contribute as so-called multi-jet background and are estimated out of data via a so-called matrix method. The previously mentioned electroweak background processes are, in contrast to that, estimated with Monte Carlo simulations. The SM contributions are compared to data and shown in Figure 1 (left) after final event selection in the electron channel for events with $m_T > 252\,\text{GeV}$.
Due to the good agreement between data and expectations, limits are set separately for the electron and the muon channel and combined afterwards assuming a common branching fraction for both final states (Figure 1 (right) shows the combined W′ limit). A single-bin likelihood analysis is performed in terms of a Bayesian ansatz to determine limits to the cross-section times branching fraction of both SSM and chiral bosons. The final lower mass limits are derived at 95 % CL using the signal cross-section for W′ at next-to-next-to-leading order (NNLO) and for W* at leading order (LO). Theoretical uncertainties from variations of the renormalisation and factorisation scales, the choice of the parton distribution function (PDF) and PDF+α_s variations are visualized as width of the predicted theory band (Figure 1 (right)). Previously placed ATLAS exclusions could be strongly improved and the observed (expected) exclusion limit on the transverse mass raised to 3.24 TeV (3.17 TeV) for a SSM W′ boson and up to 3.21 TeV (3.12 TeV) for a chiral W* boson. These results are in good agreement with the most recent published limits of the CMS Collaboration [4].

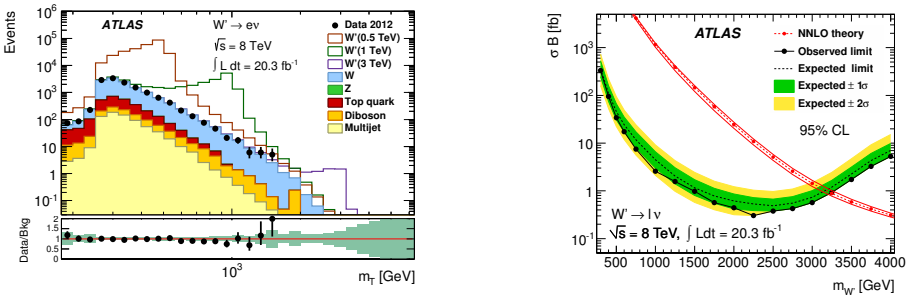

Figure 1. Transverse mass spectrum (left) after final event selection in the electron channel for events with $m_T > 252\,\text{GeV}$ and the combined W′ limit (right) [3]. The observed data is visualized as black points, compared to the coloured, stacked histograms representing the SM expectation normalized to the data luminosity. The error bars on the data points refer to statistical fluctuations. The open histograms show possible signal contributions in addition to the background processes. Predicted values for σB at NNLO are also shown (including uncertainties).

2.2 Search for heavy dilepton resonances

The next promising analysis channel to constrain various new physics scenarios considers final states with two isolated leptons [5]. The reconstructed invariant dilepton mass is chosen as signal discriminant and shown in Figure 2 (left) with a well understood background in good agreement with the observation out of data. The expected SM processes are dominated by the Drell-Yan background ($q\bar{q} \rightarrow Z/\gamma^* \rightarrow l^+l^-$), followed by diboson (WW, WZ, ZZ) and top quark production. The latter one is extrapolated to higher masses via various fits to the invariant mass spectrum. While the main background contributions are estimated out of Monte Carlo simulations using a full ATLAS detector simulation based on GEANT4, multi-jet processes are derived by a data-driven matrix method. The whole analysis uses a shape-based method determining the expected yield of signal and background events in mass bins to avoid too large background estimation uncertainties.
Due to the absence of any deviation in the high mass tail, Bayesian limits at 95 % CL are set in terms of the SSM model Z′ and the chiral Z* (see Sect. 2.1), as well as to additional modifications of the SM predicting additional Z'_χ and Z'_ψ bosons related to the existance of larger symmetry groups. Figure 2 (right) shows the observed upper limits only, since they are very similar to the expected ones. The corresponding lower mass limits for each considered model are specified as red stars. Theoretical uncertainties due to PDFs, α_s and scales are visualized as width of the Z'_{SSM} band.

A possible solution to the hierarchy problem is provided by models introducing extra-dimensions. The Randall-Sundrum model postulates one warped extra-dimension that is compactified. Its phenomenology is characterized by the mass of the lightest Kaluza-Klein excitation mode of the graviton (denoted as G*) and its coupling strength to SM particles. Despite the branching fractions to dilepton final states being small due to its spin-2 quantum number, the dilepton channel is still sensitive because of the clean signature of processes with two isolated leptons in the final states [5].
The exclusion at 95 % CL is visualized in the plane of the coupling strength of the Randall-Sundrum graviton to SM particles versus its mass (Figure 3) as the area above the curve.

Another new physics scenario is considered by the Minimal Walking Technicolor model postulating the Higgs boson as a composite particle bound by a strong force called technicolor. It provides

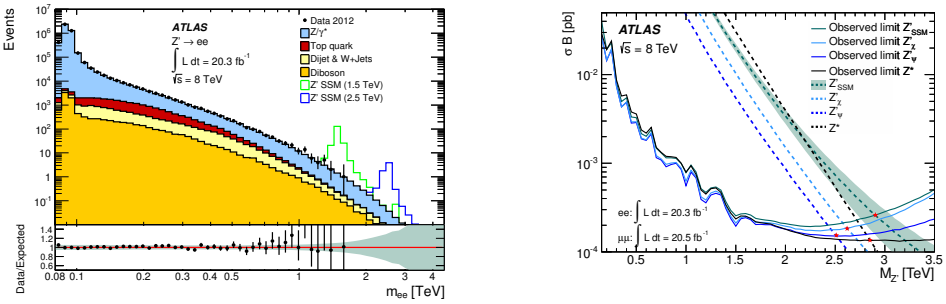

Figure 2. Invariant dilepton mass (left) and observed upper cross-section times branching ratio limits (right) at 95 % CL for various models predicting additional heavier vector-gauge bosons [5].

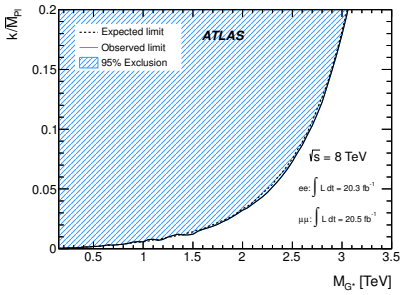

Figure 3. Expected and observed 95 % CL limits in the plane of the coupling strength of the Randall-Sundrum graviton to SM particles versus its mass for the combined electron and muon channel [5].

an alternative possible solution to the hierarchy problem by using new strong dynamics to break the electroweak symmetry and predicting new narrow technimeson resonances decaying to dilepton final states. The exactly same analysis is performed to search for any evidence to these particles but, as no excess in the invariant mass spectrum can be observed, limits to this model are provided [5]. The exclusion contours at 95 % CL in the plane of the parameter space defined by the bare axial-vector mass versus the strength of the spin-1 resonance interaction $\tilde{g}$ are shown in Figure 4 (left).

Results of the dilepton analysis are also interpreted with respect to quantum black hole (QBH) scenarios. QBH production is described within the Randall-Sundrum model but also in context of a model based on Arkani-Hamed, Dimopoulos, Dvalí (ADD). The latter one postulates n≥1 flat additional spatial dimensions that are commonly compactified with radius R. This analysis [5] assumes n=6 dimensions but the dependence of the resulting production limit on n is small. The QBH production threshold is furthermore assumed to correspond to the higher-dimensional Planck scale. The Randall-Sundrum model interpretation is approximated by the 5-dimensional ADD case. Figure 4 (right) shows the exclusion limits at 95 % CL with respect to these quantum black hole scenarios.

The presented exclusions are the most stringent to date, except for QBH production.

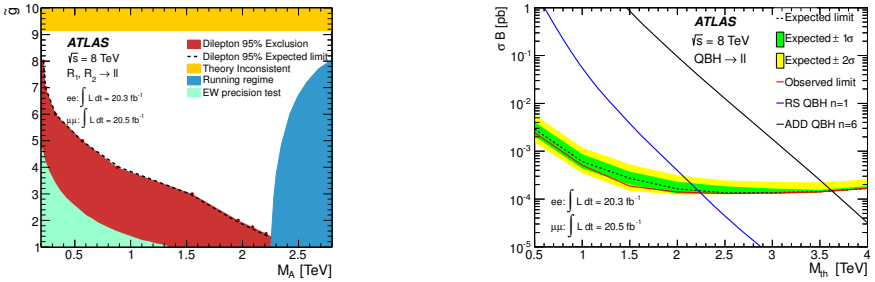

Figure 4. Exclusion contours at 95 % CL in the plane of the parameter space defined by the bare axial-vector mass versus the strength of the spin-1 resonance interaction $\tilde{g}$ are shown on the left side. Electroweak precision measurements exclude the green area; the requirement to stay in the walking regime excludes the blue one. The yellow area is excluded due to non-real axial and axial-vector decay constants. Expected and observed exclusion limits for the combined channels are visualized as the black dashed line and the red filled area [5]. The right side shows the expected and observed upper limits at 95 % CL for QBH production in context of the ADD model [5].

2.3 Search for heavy dijet resonances

Many models describe new particles created as s-channel resonances which can decay to final states involving quarks and gluons. Thus, a narrow resonance width would be visible as local excess in the dijet mass spectrum (m_{jj}).
Selecting events with two or more jets (anti-k_t, R=0.6), the dijet mass is reconstructed out of the two jets with the highest transverse momentum. The background consists mainly of QCD processes that are estimated by fitting a smooth function to the dijet mass spectrum: $f(x) = p_1(1-x)^{p_2}x^{p_3+p_4\ln(x)}$ with $x = m_{jj}$. This allows for smooth background variations but can not accomodate localized excesses. Figure 5 demonstrates the fitting procedure with the relative difference to data in the central panel and the bin-by-bin significance of the difference between data and background expectation in the bottom panel. The BumpHunter algorithm is used but no significant deviation from the SM processes can be observed. Combining promptly reconstructed data with delayed stream data (data from hadronic triggers that was recorded and reconstructed later), two independent mass distributions are reconstructed and averaged using the effective integrated luminosity as a weight. Thus, the usable luminosity can be increased by one order of magnitude and the examined dijet mass range enlarged to a range of 0.25 TeV up to 4.5 TeV.

Model-dependent as well as model-independent interpretations have been considered and limits at 95 % CL are provided in the context of excited up and down-type quarks (q^*), the production of exotic colored resonances, the SSM W′ as well as chiral bosons (W^*) and quantum black holes (QBH) [6]. The corresponding lower mass limits are summarized in the table shown in Figure 5. Model-independent limits are set using two different approaches: Firstly, resonances are assumed to have a Gaussian shape near the core with tails smaller than the background expectation. And secondly, limits are set involving resonances that approximate a Breit-Wigner shape and extend with a low-mass tail due to effects of parton luminosity. The results of these two different approaches are shown in Figure 6.

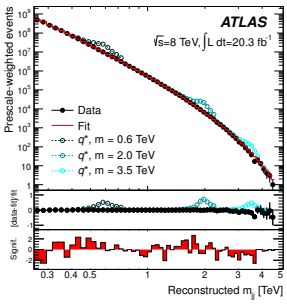

model	decay	m_{obs} [TeV]	m_{exp} [TeV]
q^*	qg	4.09	3.99
s8	gg	2.72	2.83
W′	$q\bar{q}'$	2.45	2.51
W*	$q\bar{q}'$	1.75	1.93
QBH	q, g	5.82	5.82

Figure 5. Reconstructed dijet mass spectrum (left) fitted with a smooth functional form. Predictions of three possible excited quark signals are visible above the background expectation. The relative difference between data and fit, as well as the bin-by-bin significance of the difference are shown in the lower two panels [6]. Expected (m_{exp}) and observed (m_{obs}) lower mass limits for various models are derived at 95% CL in a dijet resonance search and shown on the right side [6].

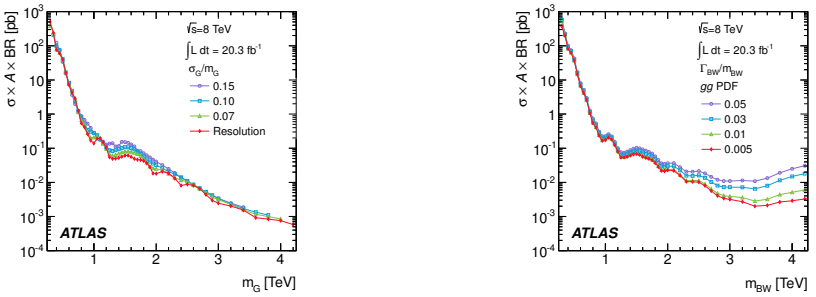

Figure 6. Upper limits at 95 % CL presented for a simple Gaussian resonance (left) and a Breit-Wigner narrow resonance each decaying to dijet final states. Statistical and systematic uncertainties are shown [6].

2.4 Search for heavy resonances decaying via a pair of Higgs bosons

A search for heavy resonances decaying to a pair of SM Higgs bosons is performed and results are interpreted in terms of the bulk Randall-Sundrum model described as above (see Sect. 2.2) [7]. The decay of a SM Higgs boson is reconstructed from a pair of b-tagged jets (anti-k_t, R=0.4) resulting in two dijet systems, each with a transverse momentum of above 200 GeV. The dijet mass should be approximately equal to the Higgs mass. The four-jet mass m_{4j} is used as signal discriminant whereby the natural width of the G* resonance should be smaller than m_{4j} (about 15 %).
The major background contribution arises due to multi-jet events. Further considered SM processes are $t\bar{t}$ production and Z+jets processes. Due to its complexity, the multi-jet background is totally estimated out of data whereas the $t\bar{t}$ contribution gets its shape out of MC simulations and the corresponding normalization from data. The tiny amount of Z+jets events (< 1 %) is estimated via MC simulations only.
Since no evidence for new physics has been observed (Figure 7 (left)), upper limits are derived at 95 % CL using the signal strength as parameter of interest and a profile likelihood ratio as test statistic. The

resulting constraints of 590 GeV $< m_{G^*} <$ 710 GeV in the mass for the Randall-Sundrum graviton are demonstrated in Figure 7 (right).

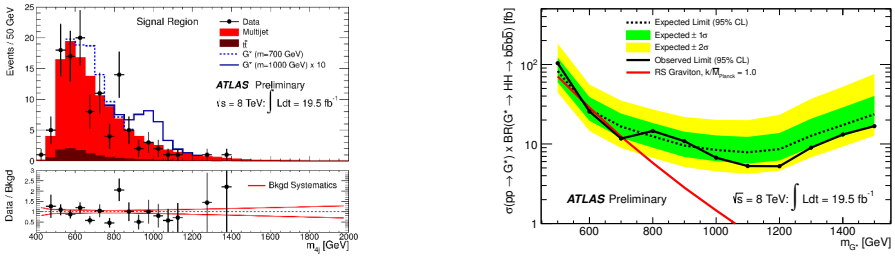

Figure 7. Comparison of observed m_{4j} data spectrum to SM expectations in the signal region (left) as well as final expected and observed 95 % CL upper limits as function of the Randall-Sundrum graviton mass (right). The LO prediction in context of the Randall-Sundrum model is also shown [7].

2.5 Search for microscopic black holes in final states with leptons and jets

Searching for microscopic black holes, final states including ensembles of high-energy particles are examined [8]. The production threshold for such black holes is assumed to be well above the fundamental gravitational scale in the full (n+4) space-time dimensions. Once such black holes have formed and settled into non-rotating (Schwarzschild) or rotating (Myers) states, they are assumed to loose their mass and angular momentum through emission of Hawking radiation while emitting all types of SM particles. The emission energy spectrum is characterized by the so-called Hawking temperature and therefore not a pure black-body spectrum.
Since branching fractions to final states with at least one lepton are between 15-50 %, events with at least three high-p_T objects including at least one lepton and the sum of transverse momenta ($\sum p_T$) above 2000 GeV are selected. Dominant background processes are W or Z plus jet events, followed by $t\bar{t}$ production and multi-jet processes. The latter ones are estimated via a data-driven matrix method while the former are derived out of MC simulations and extrapolated to high $\sum p_T$ regions.
The dominant systematics are due to the fitting uncertainty whereas the most important experimental uncertainty arises due to in situ techniques used for the jet energy scale.
Since no evidence for new physics can be observed, frequentistic CLs limits are set on a fiducial cross-section (defined as the part of the total cross-section within kinematic restrictions)[3] as well as on TeV-scale gravity benchmark models using a profile likelihood ratio as test statistic. Figure 8 demonstrates a stronger exclusion for an increasing number of extra dimensions due to larger signal cross-sections, as well as for non-rotating systems because of the increasing number of Hawking emissions. The limits provided are the strongest published ATLAS exclusions and represent, together with those placed by CMS, the most stringent bounds on the considered models.

[3] $\sigma_{fid} = \frac{N_{sig}}{L_{int} \cdot c}$ where c is a reconstruction efficiency factor

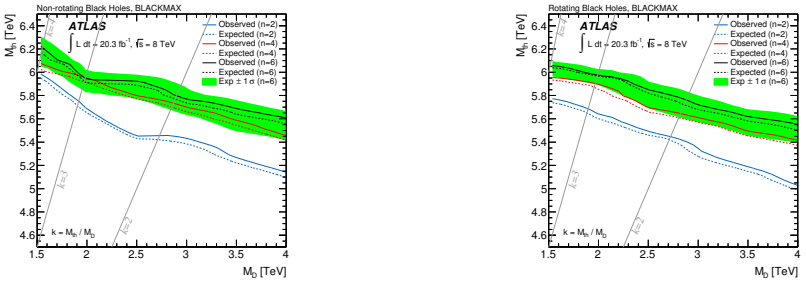

Figure 8. Combined expected and observed limits at 95 % CL for non-rotating (left) and rotating (right) black hole models simulated with Blackmax. Two, four and six extra dimensions are considered whereby the expected 1σ deviation is shown for n=6 only (comparable for n=2, n=4) [8].

2.6 Search for quantum black hole production in lepton+jet final states

Evolving black holes lead to a decrease in mass and quantum gravitational effects become important. As theoretical modelling uncertainties are large, QBH remnants are simulated conventionally decaying to a small number of SM particles and a search is performed, for example, in lepton+jet final states [9]. The results are interpreted in context of the ADD model described in Sect. 2.2. The mass reconstructed out of one lepton and the jet with the highest transverse momentum (anti-k_t, R=0.4) is used as signal discriminant (Figure 9 (left)). SM background contributions arise out of vector-boson production with additional jets, diboson (WW, WZ, ZZ), top pair and single top production (known as electroweak (EW) background) as well as out of multi-jet processes. Data control regions ($440 < m_{e,jet} < 900$ GeV) are used for normalisation of the Monte Carlo (EW) and data-driven (multi-jet) background estimates that are extrapolated afterwards to higher masses via fits. The systematic uncertainty in this analysis is dominated by fit and PDF uncertainties.
Due to absence of a significant excess over the smooth SM expectation, upper limits for QBH production above a minimal threshold mass between 1-6 TeV are derived at 95 % CL via a CLs method (Figure 9 (right)). Lepton universality is assumed. The search presented is the first for two body lepton+jet final states with large invariant mass.

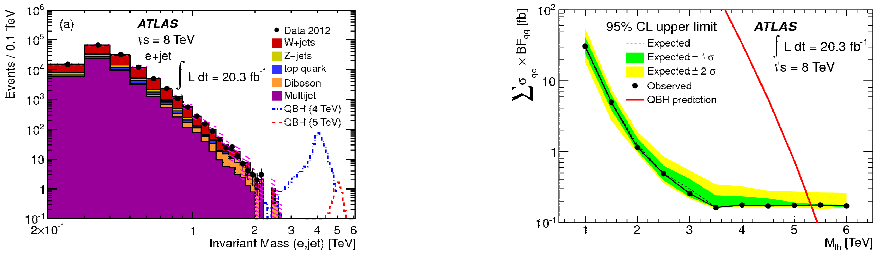

Figure 9. Invariant mass spectrum reconstructed out of one electron here and the highest-p_T jet (left). The hatched area visualizes statistical and systematic uncertainties. The combined expected and observed 95 % CL upper limits are shown on the right side. The predicted cross-section for QBH is visualized as solid line [9].

2.7 Search for quantum black hole production in photon+jet final states

The last search considered for non-thermal quantum black hole production is performed in photon+jet final states and results are interpreted in context of the ADD model (described in Sect. 2.2) [10]. Final states with one high-p_T photon plus an additional jet (anti-k$_t$, R=0.6) are analysed. The reconstructed photon plus jet invariant mass is used as signal discriminant that shows a smooth and rapidly falling behavior for masses above 426 GeV due to a mixture of direct and secondary γ+ jet production. Underlying SM background processes are estimated by fitting the data, similar to the dijet analysis, with the functional form $f(x) = p_1(1-x)^{p_2}x^{-(p_3+p_4 \ln x)}$ ($x = m_{\gamma j}$) and validated within two additional control samples: The BumpHunter algorithm is used to calculate the bin-by-bin significance whereby the fit quality is quantified using a negative log-likelihood test statistic.
Since no resonant excesses have been observed (Figure 10 (left)), Bayesian limits are provided at 95 % CL and QBH with masses up to 4.6 TeV excluded (Figure 10 (right)). This is the most stringent exclusion placed to date for the production of new resonances in the photon+jet final state.

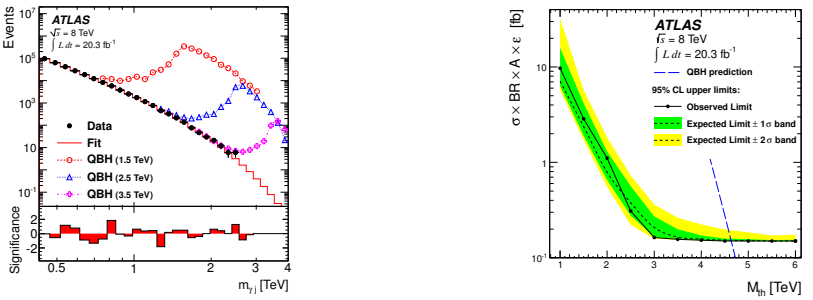

Figure 10. Invariant γ+ jet mass spectrum fitted with a smooth functional form (left). The bin-by-bin significance of the difference between data and fit are shown. The 95 % CL upper limits can be seen on the right side [10].

2.8 Contact interactions (CI)

Finally, it is worth mentioning that new phenomena might be not always visible as narrow resonances but possibly also as broad deviations from the SM. Thus, the last considered analysis searches for new interactions in the dilepton channel at scales higher than directly accessible in resonance searches [11]. Such interactions are described as so-called "four-fermion contact interactions" (as suggested by Fermi). The CI search is performed in six broad mass bins (within the signal region) using both the invariant dilepton mass and the dilepton decay angle (defined in the Collin-Soper frame) as signal discriminant.
The largest (irreducible) background contribution arises due to Drell-Yell and photon-induced processes, followed by top production, multi-jet, W+jets and diboson decays. Multi-jet and W+jets background events are estimated via a data-driven fake-factor method and extrapolated to higher masses (as well as the top processes).
In terms of a Bayesian approach, lower limits on the characteristic energy scale Λ are derived at 95 % CL and shown for various models in Figure 11. The most restrictive exclusion is obtained in the combined dielectron and dimuon channel for the left-right CI model with constructive interference and a prior flat in $1/\Lambda^2$.

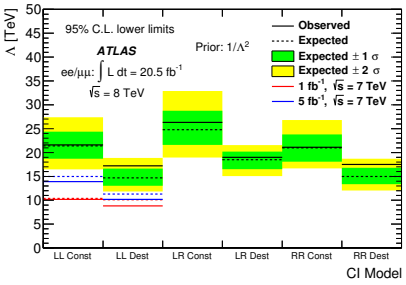

Figure 11. Summary of 95 % CL lower exclusion limits on the characteristic CI energy scale Λ for the combined electron and muon channel [11].

3 Conclusion

Proton-proton collision data recorded in 2012 with the ATLAS detector at a center-of-mass energy of $\sqrt{s}$ =8 TeV and a corresponding integrated luminosity of about L_{int} ≈20 fb^{-1} has been analysed and the most recent results on searches for new physics beyond the SM were presented. Due to absence of any evidence for new physics scenarios, limits to various models were derived at 95 % CL. Previously placed ATLAS exclusions could be strongly improved and in many cases the most stringent limits to date are provided. Considered are heavy vector gauge bosons, chiral bosons as well as excited quarks and technicolor, a Randall-Sundrum graviton, the ADD large extra dimension scenario, (quantum) black holes and contact interactions.

References

[1] L. Evans and P. Bryant (editors), JINST **3** S08001 (2008).
[2] ATLAS Collaboration, JINST **3** S08003 (2008).
[3] ATLAS Collaboration, JHEP **09**, 037 (2014), arXiv:1407.7494.
[4] CMS Collaboration, PRD **87**, 072005 (2013), arXiv:1302.2812.
[5] ATLAS Collaboration, PRD **90**, 052005 (2014), arXiv:1405.4123.
[6] ATLAS Collaboration, arXiv:1407.1376, submitted to PRD.
[7] ATLAS Collaboration, ATLAS-CONF-2014-005, http://cds.cern.ch/record/1666518/files/ATLAS-CONF-2014-005.pdf.
[8] ATLAS Collaboration, JHEP **08**, 103 (2014), arXiv:1405.4254.
[9] ATLAS Collaboration, PRL **112**, 091804 (2014), arXiv:1311.2006.
[10] ATLAS Collaboration, PLB **728**, 562 (2013), arXiv:1309.3230.
[11] ATLAS Collaboration, arXiv:1407.2410, submitted to EPJC.